Partial Discharge Detection for Evaluation of Insulation Integrity in Aerospace Electric Power System Wiring and Components

D. L. Schweickart, Air Force Research Laboratory, WPAFB, Ohio 45433, USA
D. F. Grosjean, Innovative Scientific Solutions, ISSI, Dayton, Ohio 45440, USA
X. Liu, D. G. Kasten, S. A. Sebo
Department of Electrical and Computer Engineering, The Ohio State University, Columbus, Ohio 43210, USA

Abstract- **The paper describes the importance of partial discharge (PD) detection for aerospace electric power system wiring and components in low pressure environment. The relationships between recorded discharge pulse current waveforms and PD electrical characteristics are explained and discussed. Features of a new PD analyzer for low pressure applications are reviewed.**

I. Introduction

The reliable performance and proper functioning of electric power system components and subassemblies under operating conditions are critical features for the operation and survival of aerospace vehicles. Consequently, the behavior of the electrical insulation under such operating conditions, i.e., in a reduced- pressure environment, is critical.

Several experiment series have been conducted in air, argon and helium, in order to identify and obtain relevant test parameters for partial discharge (PD) detection. These tests have provided information towards the design and development of a prototype PD detection system for low pressure applications [1].

The energized electrode (point, loop or one of the conductors) was subjected to power frequency (60 Hz) high voltage. Tests with dc energization were also carried out. All tests were conducted for pressures in the range of 266 Pa to 101.3 kPa (2 to 760 Torr), corresponding to a range of altitudes of about 40 km (130 kft) to sea level.

The discharge current pulse waveform was captured for each PD event, utilizing a 50-ohm viewing resistor. The variations of these waveforms, for a specific combination of electrode shape, gas environment, and source voltage type, were organized and evaluated. The evaluation criteria included the waveform polarity, magnitude, rise time, frequency components, phase angle (temporal location) relative to the source voltage, time integration of the waveform (charge content), and waveform parameter statistical distributions. Each one of these features can be correlated with the pressure.

A PD detection system is being developed for use with a vacuum chamber. The system has a data acquisition and recording subsystem, and another subsystem with some on-line intelligence that analyzes the test results as the test is being conducted. A rugged PC with a fast analog-to-digital (A/D) converter card is utilized. Appropriate waveform-analysis software that considers the pressure (i.e., altitude) is utilized. Both time-domain and frequency-domain approaches are included in the data analysis. Various tools for handling the data, such as statistical, FFT, and wavelet analysis, are being investigated.

II. Recorded Waveforms and PD Electrical Characteristics

Partial discharges are electrical breakdowns within an insulating medium that do not completely bridge the space between conductors. In electrical-insulating systems, the most common occurrences of PD are field-enhanced discharges at a sharp point of a conductor (often referred to as corona), and an avalanche-type discharge within a gaseous space where a solid or liquid insulation prevents the discharge from fully extending between the electrodes.

PD is unwanted in insulating systems. Although a limited number of occurrences of partial breakdown do not generally affect the integrity of an electrical insulation system, repeated PD will degrade the performance, resulting in eventual failure. Even if complete "shorting" of insulated conductors does not occur, side effects such as an abundance of electromagnetic interference, and heat damage to neighboring wires and components can be catastrophic.

Qualification testing of electrical-insulating systems that will operate under moderate-to-high voltage stresses generally includes testing for the presence of PD [2]. Also, because voids and delaminations within solid or liquid insulating systems are indicative of defective fabrication or deterioration, insulating systems are sometimes subjected to testing for PD at voltages above normal operating potentials. Typically, total charge transferred in the conductors as a result of PD in the insulation is used as a measure of the extent of the PD event. Measurement of this "apparent charge" or "apparent PD" does not require high-bandwidth instrumentation, and is the generally accepted technique [2].

Project is supported by the USAF-SBIR Program under contract FA8650-04-C-2485.

Report Documentation Page

Form Approved
OMB No. 0704-0188

1. REPORT DATE	2. REPORT TYPE	3. DATES COVERED
01 MAY 2006	**N/A**	**-**

4. TITLE AND SUBTITLE	5a. CONTRACT NUMBER
Partial Discharge Detection for Evaluation of Insulation Integrity in Aerospace Electric Power System Wiring and Components	5b. GRANT NUMBER
	5c. PROGRAM ELEMENT NUMBER
6. AUTHOR(S)	5d. PROJECT NUMBER
	5e. TASK NUMBER
	5f. WORK UNIT NUMBER
7. PERFORMING ORGANIZATION NAME(S) AND ADDRESS(ES) **Air Force Research Laboratory, WPAFB, Ohio 45433, USA**	8. PERFORMING ORGANIZATION REPORT NUMBER
9. SPONSORING/MONITORING AGENCY NAME(S) AND ADDRESS(ES)	10. SPONSOR/MONITOR'S ACRONYM(S)
	11. SPONSOR/MONITOR'S REPORT NUMBER(S)

12. DISTRIBUTION/AVAILABILITY STATEMENT
Approved for public release, distribution unlimited

13. SUPPLEMENTARY NOTES
See also ADM001963. IEEE International Power Modulator Symposium (27th) and High-Voltage Workshop Held in Washington, DC on May 14-18, 2006, The original document contains color images.

14. ABSTRACT

15. SUBJECT TERMS

16. SECURITY CLASSIFICATION OF:			17. LIMITATION OF ABSTRACT	18. NUMBER OF PAGES	19a. NAME OF RESPONSIBLE PERSON
a. REPORT	b. ABSTRACT	c. THIS PAGE			
unclassified	**unclassified**	**unclassified**	**UU**	**5**	

Standard Form 298 (Rev. 8-98)
Prescribed by ANSI Std Z39-18

The recent availability of economical, high-speed instrumentation, such as high-digitizing-rate oscilloscopes and plug-in cards for desktop computers, has led to the widespread ability to record waveforms at frequencies over 200 MHz. This high-bandwidth capability allows for the extraction of more information than the apparent-charge measurement, but circuit limitations must be understood in order to properly interpret recorded waveforms.

To illustrate the effects of circuit parameters, some recorded waveforms of PD within a shielded, two-conductor cable will be analyzed below with the aid of circuit simulation. The cable is used in a high-voltage flashlamp circuit. The cable consists of two insulated conductors located within a conductive sheath. Distance between end connectors is about 45 cm.

For testing purposes, the cable is formed in a circular shape such that the two connectors are within approximately five cm of each other, and the corresponding conductors are connected externally; no conductors are open-ended. Fig. 1 illustrates the connections. One conductor is designated as the "test" conductor and is connected to the high-voltage source through a 200-kohm ballast resistor. The other conductor is connected to the shield and then "grounded" through a 50-ohm coaxial load. The oscilloscope is connected parallel to the load via 50-ohm coaxial cable with an additional 50-ohm load at the oscilloscope input. This combination of 50-ohm resistors and cable results in a 25-ohm effective current-viewing resistance (CVR) with minimal signal distortion.

Fig. 2 shows typical current waveforms for PD with the cable in air at various pressures. The high-frequency oscillation (about 19 MHz) is present at all displayed pressures. This oscillation disappears at pressures less than 0.4 kPa, but pressures under 0.67 kPa (5 Torr) correspond to flight altitudes of over 33.5 km (110 kft), and are not of interest at this time.

For circuit simulation, an effective alternative to complicated gas-kinetic modeling of the partial discharge is a voltage-dependent current source or, more simply, a time-varying resistance. Prior to a discharge, the effect of the circuit on the electric field distribution for the cable of Fig. 1 can be modeled as a set of capacitances. If the geometry of the conductors and insulators is uniform, the voltage at the gap is well defined by distribution of the electric field. If imperfections are present, the electric field strength will be larger at some locations than at others.

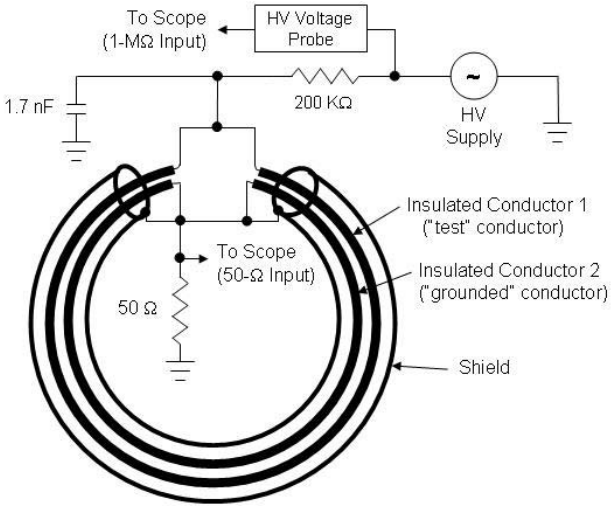

Fig. 1. Schematic diagram of setup for PD testing of flashlamp cable.

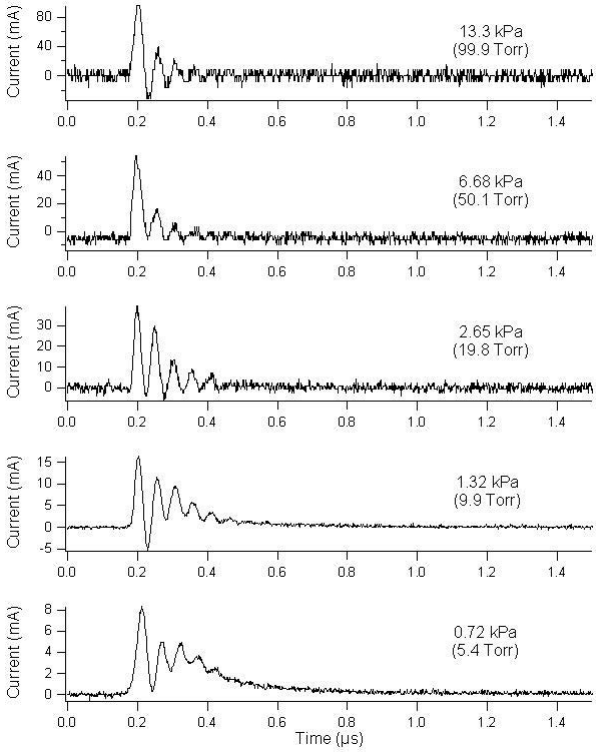

Fig. 2. Typical recorded PD current waveforms in air at various pressures.

When a section of an insulator breaks down, the electric field in the vicinity of the discharge will be distorted and the distribution of effective capacitances will vary. The interested reader is referred to excellent discussions by McAllister [3] and Pedersen [4] on details of the physics of the distribution of fields and charges.

A simple method for determining time-changing currents and voltages of an electrical circuit is simulation with a SPICE -based computer-software package. Commercially available routines do not generally allow for time-changing capacitances, but some will handle time-dependent resistances. A practical approximation to the discharge model, then, becomes a time-varying resistance in series with a capacitance. A SPICE model with a time-dependent resistance is used for the remainder of the analysis below.

Prior to gap breakdown (PD event), the actual voltage at the gap is determined by (1) the electric-field distribution, (2) leakage currents, (3) the applied voltage, and (4) the rate at which the applied voltage varies. If breakdown voltage is to be predicted, it is necessary to determine values of leakage resistances and capacitances. If the goal of the analysis,

however, is an explanation of measured current waveforms, it is generally necessary to know only the voltage between conductors at the time of breakdown. In a testing configuration, that voltage is typically measured [2].

Simulation of a measured response after gap breakdown for the setup of Fig. 1 can best be modeled with discrete components as shown in Fig. 3. For the example here, a 200-kohm resistor is used as the power-source ballast resistor ($R_{Ballast}$). The peaking capacitor (C_P) is a 1.7-nF door-knob type. R_{Gap} represents the time-varying resistance of the PD, C_2 is the lumped-element equivalent capacitance in series with the discharge, and C_{1b} represents the cable capacitance that is undisturbed by the discharge. Capacitance (C_{1a}, not shown) of the cable prior to PD was measured to be 79 pF. Stray inductances of the cable are estimated to be 100 nH at the gap (L_2), and 200 nH away from the gap (L_1). In reality, the cable inductance is distributed, but the use of two lumped elements is an approximation that helps to visualize the circuit operation. The inductance (L_3) of the connection between the cable and a 25-ohm effective CVR is estimated to be 800 nH. The cable is located within a vacuum bell-jar with separate vacuum feedthroughs for the high-voltage source conductor and the low-potential return conductor. The peaking capacitor (C_p) and the current-viewing resistances are located external to the chamber.

The capacitance (C_2 of Fig. 3) in series with the gap (R_{Gap}) must be sufficiently large that the CVR current is not reduced below that observed. Repeating simulations with various values of C_2 will indicate the minimum value. This procedure will aid in estimating the spatial extent of PD.

The critical element in simulating observed waveforms is the time-varying resistance of R_{Gap}. The procedure employed for the cable under test was (1) set C_2 at a relatively large value of about 20 pF; (2) assume an initial large value of R_{Gap}, then vary the fall time, minimum value, and rise time of R_{Gap} until the current of R_{CVR} matches the current waveforms recorded during actual PD events; and (3) reducing the value of C_2 to the point at which the current waveform begins to be affected. The resulting current of the R_{Gap} branch is a good approximation of the actual conductor current in the vicinity of the gap, and provides insight into the actual PD event.

At each half cycle of the energizing voltage, capacitors C_P and C_{1b} acquire charge. For the example here, and for many components tested with 60-Hz power, the rate-of-change of currents and voltages prior to PD are sufficiently small that

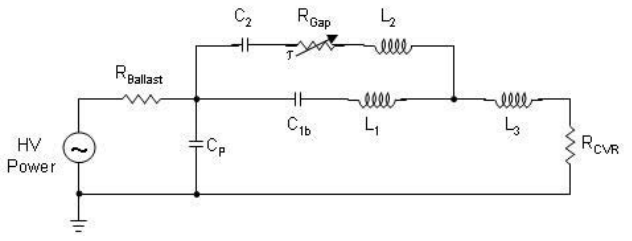

Fig. 3. Equivalent lumped-element circuit for SPICE analysis of PD in cable-test setup of Fig. 1.

inductor voltages are insignificant and the voltages on C_P and C_{1b} mimic the power voltage. While the gap is conducting, current flows through C_2, R_{Gap}, and L_2, and then is divided among the circuit branch consisting of C_{1b} and L_1, and the branch consisting of L_3, R_{CVR} and C_P. The stored charge of C_P and C_{1b} supplies the charge for the "effective" gap current. The relative values of L_1 and L_3 determine, for the most part, the relative currents of their respective branches during fast breakdown.

Because of the widely different impedances of the two branches, the temporal characteristics of the R_{CVR} circuit branch during gap conduction will exhibit a high frequency oscillation superimposed on a low-frequency oscillation. If the gap conducts for a time period that is short compared to the period of the oscillation of the low-frequency branch (L_3, R_{CVR} and C_P), the low-frequency oscillation is not observed. In addition, the power dissipated by the resistive elements may cause a damping of the oscillation. C_{1b} and L_1 constitute the high-frequency branch.

The high-speed oscillations of Fig. 2 are a result of the gap conducting for a very brief period of time. That is, an electrical breakdown in the gaseous gap effects a fast-rising current in the conductors, followed by a space-charge buildup within the gap that terminates conduction, resulting in a fast-rising, short-time-duration current in the gap branch of the equivalent circuit (Fig. 3). Essentially, charge flowing in the vicinity of the gap -- and reaching the cable ends -- during the short conduction time "charges" the monitor-circuit loop consisting of C_P, C_{1b}, L_1, L_3, and R_{CVR}. This loop then exhibits a damped oscillation consistent with the values of the circuit elements and the voltages and currents existing at the time that the gap ceases conduction. The frequency is dominated by the small capacitance of C_{1b}, along with small inductances.

If the gap remains in conduction for a significant time, the characteristic frequency would be dominated by the circuit loop consisting of C_P, C_2, R_{GAP}, L_2, L_3, and R_{CVR}. The lower pressure CVR-current waveforms of Fig. 2 appear to have low-frequency and high-frequency components; the higher-pressure waveforms appear to exhibit primarily the high-frequency component. Therefore, at high pressures, the gap conducting time is short and the high-frequency branch (C_{1b}, L_1) of the circuit is dominant. Gap conduction time is significantly longer at 0.72 kPa (5.4 Torr) than at 13.3 kPa (99.9 Torr), and some effect of increased conduction time appears to be present at 6.68 kPa (50.1 Torr).

Figs. 4-6 show results of adjusting the gap resistance in order to approximate the measured CVR current waveforms. The agreement of the modeled and CVR current waveforms is good. It should be possible to get even better agreement by modifying the form of the time-dependent resistances. The present trial version of the SPICE package has limited flexibility in altering internal models. However, the results are instructive.

The CVR current waveform of the 13.3-kPa (99.9-Torr) case (Fig. 4) is nearly symmetric about the zero-current axis, except for the initial positive spike. This is indicative of a fast charge transfer from the loop containing the PD to the oscillating loop

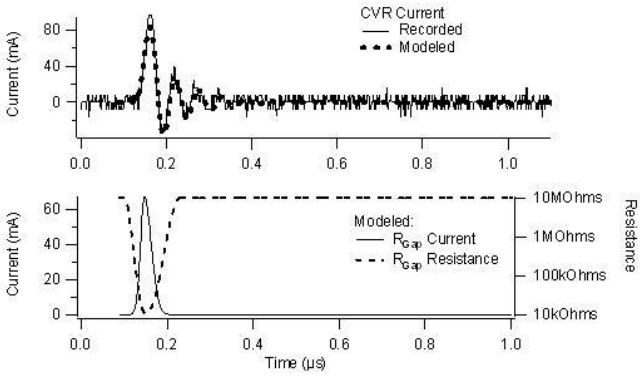

Fig. 4. Comparison of recorded CVR current at 13.3 kPa (99.9 Torr) and modeled R_{CVR} current (top plot) resulting from modeled R_{Gap} resistance and R_{Gap} current (bottom plot).

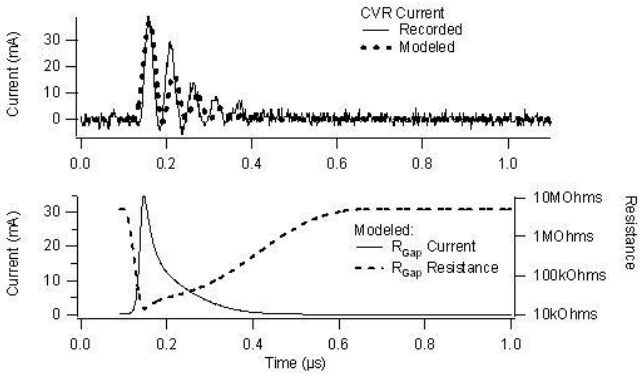

Fig. 5. Comparison of recorded CVR current at 2.65 kPa (19.8 Torr) and modeled R_{CVR} current (top plot) resulting from modeled R_{Gap} resistance and R_{Gap} current (bottom plot).

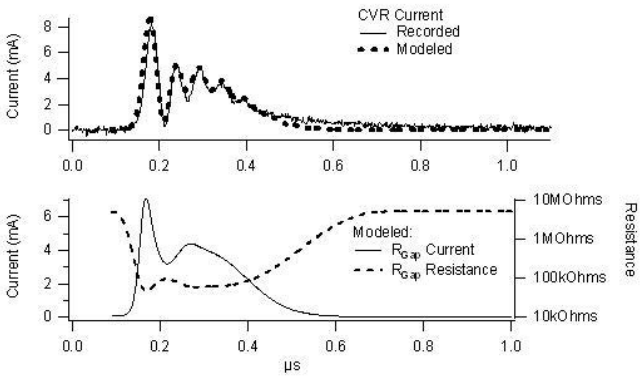

Fig. 6. Comparison of recorded CVR current at 0.72 kPa (5.4 Torr) and modeled R_{CVR} current (top plot) resulting from modeled R_{Gap} resistance and R_{Gap} current (bottom plot).

that is observed via R_{CVR}. The symmetry results from the PD loop being non-conductive during the damped oscillation.

The amplitude of the observed waveform gives some insight into the initial PD spike. If the time of the PD spike was very short compared to the time of the oscillation half-cycle, the observed initial spike would be consistent with the damped oscillation. In this case, the peaks of each positive half-cycle are about 50 % of the previous peak, so the first peak would be about twice the second positive peak. In reality, the first peak is about three times the second peak. Effectively, the PD circuit is conducting for a portion of the first half-cycle.

The CVR current waveform at 2.65 kPa (19.8 Torr) indicates longer effective gap-conduction time (Fig. 5) than encountered at higher pressure. The oscillation is non-symmetric about the zero-current axis, dropping below the axis for only short periods of two half-cycles. This is a result of the extended tail of the gap current. That is, the gap exhibits finite conduction for numerous oscillation cycles.

The 0.72 kPa (5.4 Torr) CVR current waveform of Fig. 6 shows that the gap conduction time increases even further as the pressure decreases. The oscillation is present, indicating that the circuit loop containing R_{CVR} is "charged" by an initial fast-rising gap current. Also, the oscillation is entirely one polarity, indicating that the R_{Gap} continues to conduct well beyond the time of one half-cycle. In addition, the conducting tail appears to actually increase conduction following a R_{Gap}-current decrease.

At this point, the extent of the discharge can be estimated. The current observed in the R_{CVR} loop is a result of a movement of charge in the overall circuit, initiated by movement of charge in the gap circuit branch. As charge moves in this branch, the voltage of the capacitance (C_2 of Fig. 3) in series with the gap will change. This voltage will reduce the voltage on R_{Gap} and reduce the gap current. The value of the series capacitance effectively determines the maximum integrated current (total charge) that can flow during the R_{Gap}-conducting time.

For the cable circuit as modeled in Fig. 3, a value of about 12 pF for C_2 will limit the current of the gap loop and effect the overall circuit to an extent that the recorded CVR current waveform cannot be simulated in the low-pressure cases. This value of capacitance represents a physical length of about 7 cm of the 45-cm-long, 79-pF cable. The high-pressure (13.3-kPa or 99.9-Torr) case can be simulated with a capacitance of over 4 pF, representing a possible length of about 2.3 cm of the cable.

Because of the relatively smooth shape of the tail of the effective gap current, the extended conduction time is likely due to a geometrically extended Townsend-like discharge that is affected by UV and charged particles of an initial streamer-like discharge. Caution must be exercised at this point in the use of discharge terminology. Tanaka [5] describes swarming micro-discharges as very small-amplitude PD in a gap consisting of a metal electrode and insulator. Bartnikas and Novak [6] suggest the term "pseudoglow" to describe this type of discharge because of characteristics that imply a cross between the mechanisms of Townsend (electron avalanche in gas volume) and streamer (electron avalanche followed by UV-initiated breakdown). See Danikas [7] for an excellent discussion on PD terminology.

Although the circuit model implies a current at the gap, it is not possible to know exactly what the gap discharge actually looks like. Only the effect on the cable loop and resulting effect at R_{CVR} is known for certain. However, the above model points out that (1) the pulse width of the disturbance is short at high pressures and increases significantly as the pressure is reduced, and (2) the length of the cable that is involved in the disturbance is greater at low pressures than at high pressures.

III. β-TEST VERSION OF PARTIAL-DISCHARGE ANALYZER

Development of the β-Test version of the Partial-Discharge Analyzer is nearing completion. The primary goal of this effort has been to produce an instrument that is capable of accurate acquisition and analysis of partial-discharge (PD) information, with minimal operator effort. To accomplish this, complete current and voltage waveforms are recorded with sufficient speed and timing resolution to extract meaningful time-dependent data for subsequent processing and statistical analysis for low pressure applications.

The present operating mode assumes a sinusoidal excitation voltage. Input signals consist of (1) a voltage-divider connection with a 1-Mohm input impedance that typically acts as the low side of a 1000:1 divider, and (2) current input represented by the voltage on a 25-ohm resistance in series with the device under test. Current-waveform signal distortion and RFI interference are minimized through the use of 50-ohm coaxial cables and terminations.

The instrument is a ruggedized, portable personal computer (PC) with an integral flat-panel monitor, keyboard, and high- and low-speed digitizing interfaces. The only requirements for operation are that the PC power line be connected to a 115-220 VAC, single-phase 50-60 Hz power source, and that the voltage input and the current input be connected to the excitation-voltage source and the low-potential side of the device under test, respectively.

Setup is accomplished with the aid of a near-real-time display of waveforms. PD rate (counts/s) is available in a rolling-time-chart format. The optimal combination of current range and trigger levels can be set with this group of controls and displays.

The integral PC keyboard is used for range and trigger inputs and to make numerical and text entries for device-under-test part number, serial number, comments, and gas pressure. Also, the acquisition time (in s) is set with a numerical entry.

The current and voltage waveforms of all triggered PD events are recorded with a high-speed digitizer at a 200-MHz rate. In addition, a low-speed digitizer records the excitation (60-Hz) waveform.

Upon successful acquisition of a data set, the PD Analyzer proceeds to the analysis section. A 3-D histogram of selected parameters as a function of phase angle (0-359 deg) of PD occurrence in the excitation waveform is displayed. Presently, plot selections include charge, rise time, pulse width measured at 50% of maximum-current height, pulse width measured at 20% of maximum-current height, and peak current.

Individual recorded waveforms can also be observed. The time scale of this plot is cursor adjustable. In addition to displaying the data acquired immediately prior to entering the acquisition section, one may also examine and re-analyze historical data.

IV. CONCLUSIONS

The PD evaluation method being developed does not supersede the application of conventional IEC and IEEE standards, but, based on the availability of PD characteristics during a specific test, will help to better determine the component pass/fail criteria for low-pressure PD testing. The results of this project will be used to review the procedures of the appropriate standards, and submit recommendations to the appropriate professional standards committees and boards, if necessary.

REFERENCES

[1] D. G. Kasten, X. Liu, S. A. Sebo, D. F. Grosjean, D. L. Schweickart, "Partial discharge measurements in air and argon at low pressures with and without a dielectric barrier," *IEEE Trans. Diel. and El. Ins.,* vol. 12, pp. 362-373, April 2005.

[2] IEC 60270, International Standard, *High-Voltage Test Techniques - Partial Discharge Measurements,* International Electrotechnical Commission, Geneva, Switzerland, 2000.

[3] I. W. McAllister, "Electric field theory and the fallacy of void capacitance," *IEEE Trans. El. Ins.*, vol. 26, pp. 458-459, June 1991.

[4] A. Pedersen, G. C. Crichton, and I. W. McAllister, "Partial discharge detection: theoretical and practical aspects," *IEE Proc. – Sci. Meas. Technol.,* vol. 142, pp. 29-36, Jan. 1995.

[5] T. Tanaka, "Internal partial discharges and material degradation," *IEEE Trans. El. Ins.,* vol. 21, pp. 899-905, Dec. 1986.

[6] R. Bartnikas and J. P. Novak, "On the character of different forms of partial discharge and their related terminologies," *IEEE Trans. El. Ins.,* vol. 28, pp. 956-968, Dec. 1993.

[7] M. G. Danikas, "The definitions used for partial discharge phenomena," *IEEE Trans. El. Ins.,* vol. 28, pp. 1075-1081, Dec. 1993.